GROUP-III NITRIDE ETCH SELECTIVITY IN BCl_3/Cl_2 ICP PLASMAS

R. J. Shul,[*] L. Zhang,[*] C. G. Willison,[*] J. Han,[*] S. J. Pearton,[**] J. Hong,[**] C. R. Abernathy,[**] and L. F. Lester[***]

[*]Sandia National Laboratories, Albuquerque, NM 87185-0603, rjshul@sandia.gov
[**]University of Florida, Department of Materials Science and Engineering, Gainesville, FL 32611
[***]University of New Mexico, Electrical Engineering, Albuquerque, NM

Cite this article as: MRS Internet J. Nitride Semicond. Res. 4S1, G8.1 (1999).

ABSTRACT

Patterning the group-III nitrides has been challenging due to their strong bond energies and relatively inert chemical nature as compared to other compound semiconductors. Plasma etch processes have been used almost exclusively to pattern these films. The use of high-density plasma etch systems, including inductively coupled plasmas (ICP), has resulted in relatively high etch rates (often greater than 1.0 µm/min) with anisotropic profiles and smooth etch morphologies. However, the etch mechanism is often dominated by high ion bombardment energies which can minimize etch selectivity. The use of an ICP-generated BCl_3/Cl_2 plasma has yielded a highly versatile GaN etch process with rates ranging from 100 to 8000 Å/min making this plasma chemistry a prime candidate for optimization of etch selectivity. In this study, we will report ICP etch rates and selectivities for GaN, AlN, and InN as a function of BCl_3/Cl_2 flow ratios, cathode rf-power, and ICP-source power. GaN:InN and GaN:AlN etch selectivities were typically less than 7:1 and showed the strongest dependence on flow ratio. This trend may be attributed to faster GaN etch rates observed at higher concentrations of atomic Cl which was monitored using optical emission spectroscopy (OES).

INTRODUCTION

Etch selectivity for the group-III nitrides has become important as interest in high power, high temperature electronic devices has increased. For example, the formation of low resistivity ohmic contacts or a gate recess for high electron mobility transistors (HEMTs) and heterojunction bipolar transistors (HBTs) requires accurately stopping the etch on a specific contact layer. Patterning the group-III nitride films has improved significantly despite their inert chemical nature and strong bond energies primarily due to the use of high-density plasma (HDP) etch systems. HDP etch systems operate under high plasma flux conditions which improve the III-N bond breaking efficiency and the sputter desorption of etch products from the surface. Unfortunately, the best etch results i.e. anisotropic profiles, smooth surface morphology and high etch rates, are often obtained under energetic ion bombardment conditions which can minimize etch selectivity. However, by reducing the ion energy or increasing the chemical activity in the plasma, etch selectivity can often be improved.

The chemical activity of an etch process and therefore the etch characteristics can be strongly effected by the choice of reactive source gas (Cl_2, BCl_3, $SiCl_4$, IBr, BBr_3, CH_4/H_2, ICl, CHF_3 etc.).[1-15] Table I shows the boiling points of possible etch products for group-III nitride films exposed to halogen-based plasmas. Etch rates are often limited by the volatility of the group-III halogen etch product. Therefore, chlorine-, iodine-, and bromine-based chemistries are preferred to etch Ga- and Al-containing materials due to the high volatility of the etch product as

https://doi.org/10.1557/S1092578300003483 Published online by Cambridge University Press

compared to fluorine-based chemistries. Chlorine-based plasmas have been the most widely used to etch Ga-containing compound semiconductors since they are less corrosive than iodine- or bromine-based plasmas and typically yield fast rates with anisotropic, smooth etch profiles. For In-containing species, etch rates obtained in room temperature chlorine-based plasmas tend to be slow with rough surfaces due to the low volatility of the $InCl_3$ etch products and preferential loss of the group-V species. However, under high plasma flux conditions the $InCl_3$ etch products are sputtered away before they can passivate the surface resulting in improved etch rates and surface morphology.[16] Also, at elevated substrate temperatures (>130°C), the volatility of $InCl_3$ etch product increases thus improving the etch results.[17-19]

Several selectivity studies have recently been reported for the group-III nitrides.[20-26] GaN:AlN and GaN:InN etch selectivities were typically < 7:1, however Smith and co-workers reported an etch selectivity > 38:1 for GaN:AlN in an inductively coupled plasma (ICP) etch system at –20 V dc-bias.[21] Plasma chemistries can have a significant effect on etch selectivities due to the differences in volatility of the etch products.[20, 24] For example, GaN:AlN and GaN:InN etch selectivities were typically > 1:1 in Cl_2-based plasmas and < 1:1 in BCl_3-based plasmas. This was attributed to higher concentrations of reactive Cl generated in Cl_2-based plasmas as compared to BCl_3-based plasmas and thus faster GaN etch rates. Alternatively, InN and AlN etch rates showed much less dependence on the Cl concentration and were fairly comparable in Cl_2 and BCl_3-based plasmas.

The use of an ICP-generated BCl_3/Cl_2 plasma has yielded a highly versatile GaN etch process with rates ranging from 100 to 8000 Å/min[27, 28] making this plasma chemistry a prime candidate for optimization of the group-III nitride etch selectivity. In this study, we will report ICP etch rates and selectivities for GaN, AlN, and InN as a function of BCl_3/Cl_2 flow ratios, cathode rf-power, and ICP-source power.

Table I. Boiling points for possible III-N etch products in halogen-based plasmas.

Etch Products	Boiling Points (°C)
$AlCl_3$	183
AlF_3	na
AlI_3	360
$AlBr_3$	263
$GaCl_3$	201
GaF_3	1000
GaI_3	sublimes 345
$GaBr_3$	279
$InCl_3$	600
InF_3	>1200
InI_3	na
$InBr_3$	sublimes
NCl_3	<70
NI_3	explodes
NF_3	-129

https://doi.org/10.1557/S1092578300003483 Published online by Cambridge University Press

EXPERIMENT

The GaN films etched in this study were grown by metal organic chemical vapor deposition (MOCVD), whereas the AlN and InN samples were grown using metal organic-molecular beam epitaxy (MO-MBE). The ICP reactor was a load-locked Plasma-Therm SLR 770 which used a 2 MHz, 3 turn coil ICP source. All samples were mounted using a thermally conductive paste on an anodized Al carrier that was clamped to the cathode and cooled with He gas. The ion energy or dc-bias was defined by superimposing a rf-bias (13.56 MHz) on the sample. Samples were patterned with AZ-4330 photoresist. Etch rates were calculated from the depth of etched features measured with an Alpha-step stylus profilometer after the photoresist was removed. Depth measurements were taken at a minimum of 3 positions. Samples were ~1 cm^2 and were exposed to the plasma for 1 to 3 minutes. Run-to run repeatability was typically better than ±10% while the uniformity across the sample was typically better than ±5%. One exception was InN samples, which yielded a uniformity closer to ±25% due to the rough surface morphology of the as-grown sample. Surface morphology, anisotropy, and sidewall undercutting were evaluated with a scanning electron microscope (SEM). The root-mean-square (rms) surface roughness was quantified using a Digital Instruments Dimension 3000 atomic force microscope (AFM) system operating in tapping mode with Si tips.

Optical emission spectra (OES) were obtained for most of the plasma conditions reported in this paper. Due to limited optical access immediately above the sample surface, spectra were obtained through a window mounted on the top of the ICP plasma generation region. Consequently, the conclusions drawn from the OES results may be only qualitatively applicable to the conditions at the sample surface, especially where mean-free paths were sufficiently short to enable several collisions between the plasma generation region and the sample surface. Atomic emission intensities from Cl species were normalized by the intensity of the Ar emission at 750 nm to correct for variations in excitation efficiency under different plasma conditions.

RESULTS AND DISCUSSIONS

A characteristic OES spectra is shown in Figure 1 for an ICP-generated BCl_3/Cl_2 plasma under the following conditions; 2 mTorr chamber pressure, 125 W cathode rf-power with a corresponding dc-bias of -235 V, 500 W ICP-power, 32 sccm Cl_2, 8 sccm BCl_3, and 5 sccm Ar. Strong emission from excited neutral Cl^0 atoms was obtained at 726, 741, 755, 775, 808.3, and 837.5 nm. Strong emissions were also observed from excited Cl^+ species at 413 nm. This implied that both Cl neutrals and ions were prominent in the group-III nitride etch process whereas our earlier study showed only weak Cl^+ emission.[28] In general, etch rate data for GaN tracked with the Cl neutral and ion emission peaks while the AlN and InN etch rates were less dependent on Cl concentration.

Changes in the plasma gas composition can have a strong effect on the chemical-to-physical components of the etch mechanism and thus etch selectivity. In Figure 2 GaN, AlN, and InN etch rates are plotted as a function of $\%Cl_2$ in the BCl_3/Cl_2 ICP plasma. Plasma parameters were 2 mTorr pressure, 500 W ICP power, and 125 W cathode rf-power with corresponding dc-bias ranging from –230 to –285 V. The dc-bias initially increased as Cl_2 was added to the BCl_3/Ar plasma and then decreased at higher Cl_2 concentrations. GaN etch rates increased up to ~4390 Å/min at 80% Cl_2 due to higher concentrations of reactive Cl. This was confirmed using OES where the Cl^+ and Cl^0 emission intensity increased up to 80% Cl_2 (see Figure 3). Slower GaN

https://doi.org/10.1557/S1092578300003483 Published online by Cambridge University Press

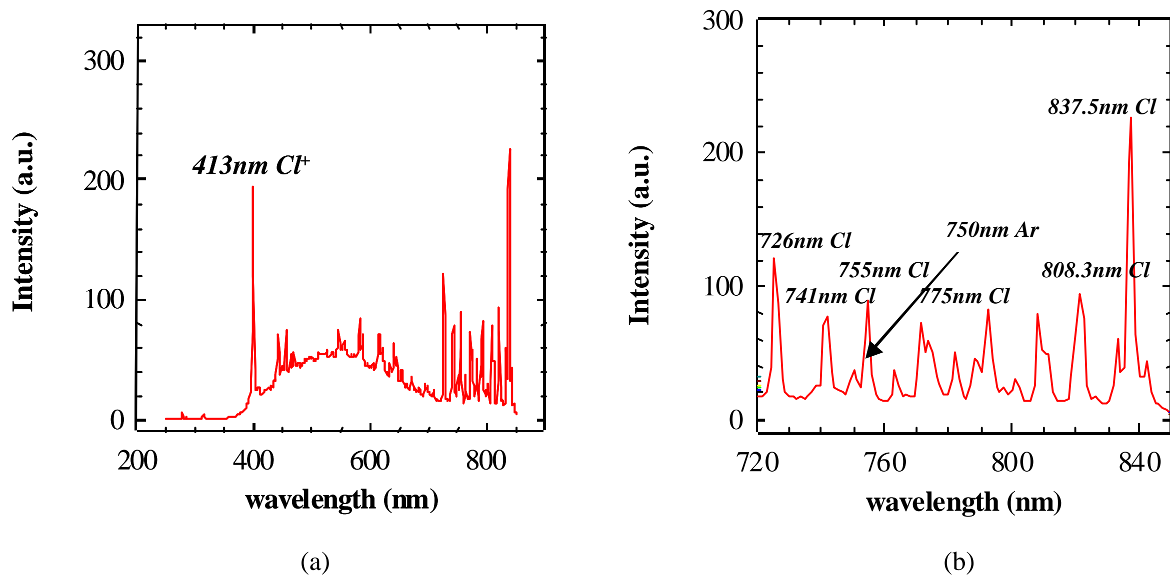

Figure 1. OES of ICP generated BCl_3/Cl_2 plasma.

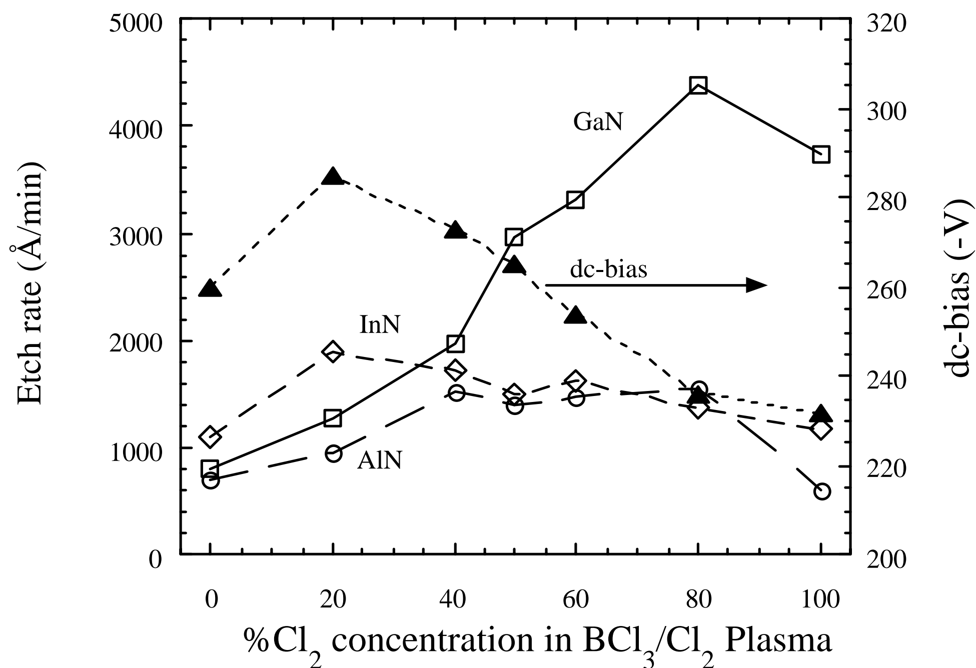

Figure 2. GaN, InN, and AlN etch rates as a function of $\%Cl_2$ in a $BCl_3/Cl_2/Ar$ ICP plasma. Plasma conditions were: 2 mTorr pressure, 500 W ICP-source power, 125 W cathode rf-power, and 25°C cathode temperature.

https://doi.org/10.1557/S1092578300003483 Published online by Cambridge University Press

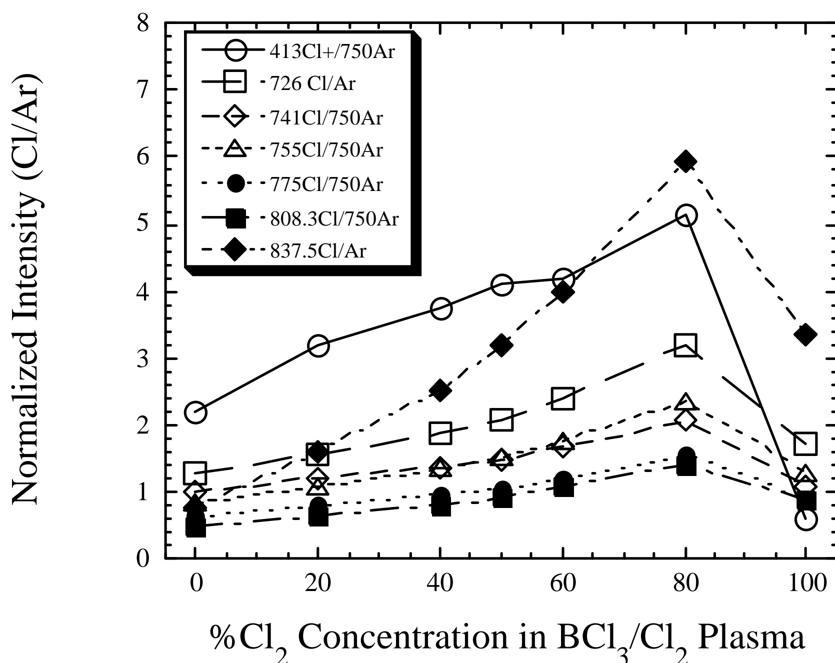

Figure 3. OES showing the increase in Cl^+ and Cl^0 emission normalized to Ar as a function of $\%Cl_2$ concentration.

etch rates observed at 100% Cl_2, were attributed to lower Cl^0 and Cl^+ emission and less efficient sputter desorption of the etch products from the surface in the absence of the heavier BCl_x ions. Lee and co-workers saw a similar trend where the maximum GaN etch rate was obtained at90% Cl_2.[14] Using OES and a Langmuir probe, they observed higher ion current densities and Cl radical densities as the $\%Cl_2$ increased.

InN etch rates initially increased as the Cl_2 concentration increased and then decreased above 20%. The AlN etch rates increased up to 40% Cl_2 concentration and then remained relatively constant. Above 50% Cl_2, InN and AlN etch rates were much slower than GaN. For InN, this may be attributed to the low volatility of the $InCl_3$ etch products, however for AlN the volatility of the $AlCl_3$ etch product is quite high. Therefore, slow AlN etch rates were attributed to their strong bond energy, 11.52 eV/atom, as compared to 8.92 eV/atom for GaN and 7.72 eV/atom for InN. The etch selectivities for GaN:AlN and GaN:InN are shown in Figure 4 as a function of %Cl concentration. In both cases the selectivities increased as the concentration of Cl_2 increased due to higher GaN etch rates. At low Cl_2 concentrations the GaN:InN selectivity was less than 1. A maximum selectivity of 6.3:1 was obtained for GaN:AlN in a pure Cl_2 plasma.

Another method of changing the chemical-to-physical component of the etch mechanism is to vary the energy of the ions which bombard the substrate surface. In Figure 5, etch rates for GaN, AlN, and InN are shown as a function of cathode rf-power (which corresponds to ion energy). Plasma etch conditions were 2 mTorr pressure, 32 sccm Cl_2, 8 sccm BCl_3, 5 sccm Ar, and 500 W ICP source power. In general, etch rates for all 3 films increased monotonically as cathode rf-power increased due to more efficient breaking of III-N bonds and sputter desorption of the etch products at higher ion energies. The decrease in etch rate for GaN at 350 W cathode rf-power may be due to sputter desorption of reactant species from the surface prior to reaction. Faster InN etch rates at higher ion energies were attributed to efficient sputter desorption of the $InCl_3$

https://doi.org/10.1557/S1092578300003483 Published online by Cambridge University Press

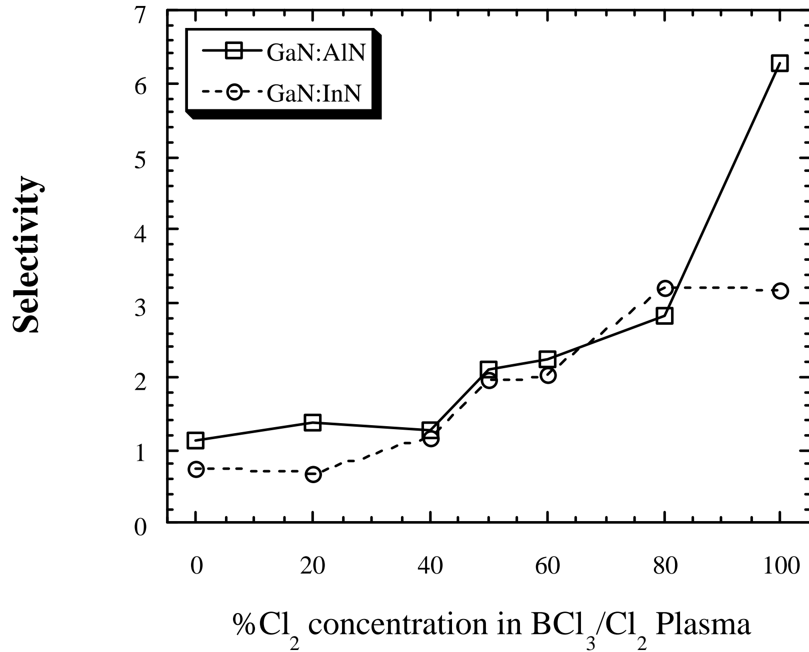

Figure 4. GaN:AlN and GaN:InN etch selectivities as a function of $\%Cl_2$ in a $BCl_3/Cl_2/Ar$ ICP plasma. Plasma conditions were: 2 mTorr pressure, ICP-source power 500 W, 125 W cathode rf-power, and 25°C cathode temperature.

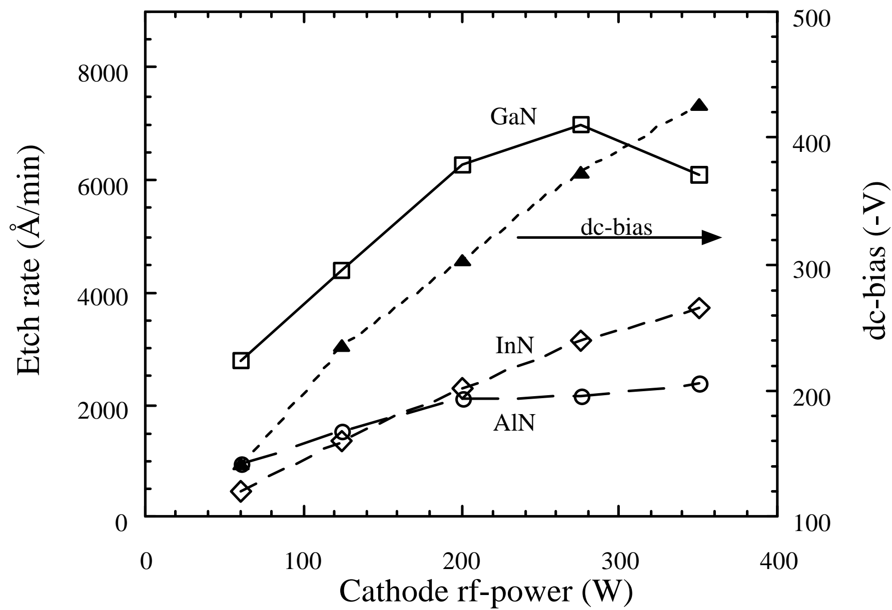

Figure 5. GaN, InN, and AlN etch rates as a function of cathode rf-power in a $BCl_3/Cl_2/Ar$ ICP plasma. Plasma conditions were: 2 mTorr pressure, ICP-source power 500 W, 32 sccm Cl_2, 8 sccm BCl_3, and 25°C cathode temperature.

https://doi.org/10.1557/S1092578300003483 Published online by Cambridge University Press

etch products prior to passivation of the etch surface by the non-volatile $InCl_3$.[16] The etch-rate dependence on dc-bias did not correlate well with Cl^0 emission intensity which was somewhat scattered over the conditions studied. However, the etch rates tracked fairly well with the Cl^+ emission intensity. Etch rates were slightly slower than our earlier results[28] due to differences in the chamber conditions as well as slightly lower dc-biases under comparable cathode rf-power. The GaN:InN etch selectivity decreased as a function of cathode rf-power (see Figure 6) due to efficient sputter desorption of the $InCl_3$ at higher ion energies. The GaN:AlN etch selectivity remained relatively constant at approximately 3:1.

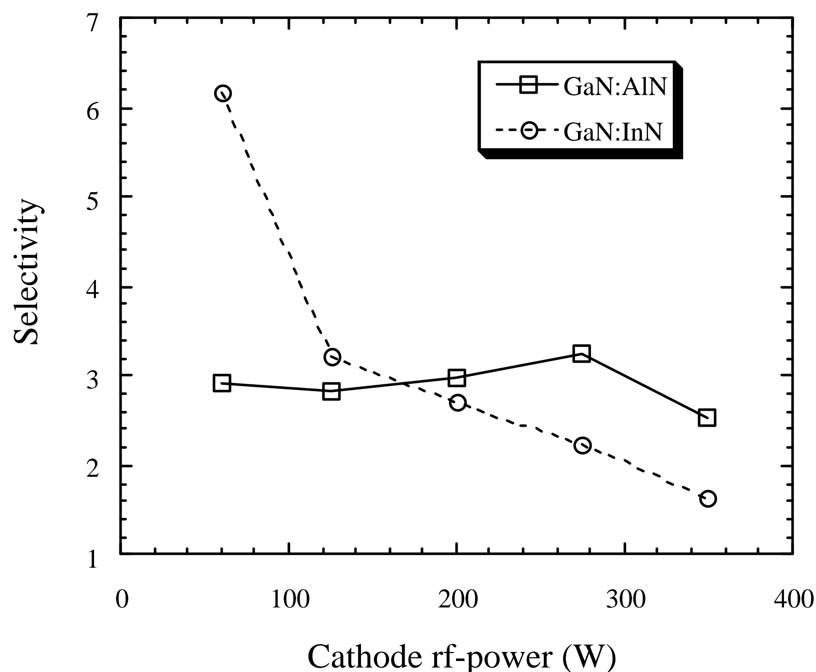

Figure 6. GaN:AlN and GaN:InN etch selectivities as a function of cathode rf-power in a $BCl_3/Cl_2/Ar$ ICP plasma. Plasma conditions were: 2 mTorr pressure, ICP-source power 500 W, 32 sccm Cl_2, 8 sccm BCl_3, and 25°C cathode temperature.

By varying the ICP source power, the chemical (reactant neutral flux) and physical (ion flux) components of the etch mechanism can be changed. As the ion flux increases so does the efficiency of III-N bond breaking and the sputter desorption of etch products from the surface. In Figure 7, GaN, InN, and AlN etch rates are plotted as a function of ICP source power. The plasma conditions were 2 mTorr pressure, 125 W cathode rf-power with corresponding dc-bias ranging from –160 to –300 V, 32 sccm Cl_2, and 8 sccm BCl_3. For all 3 films the etch rate initially increased up to 500 W ICP source power and then stabilized and even decreased at higher powers. The decrease in etch rate may be attributed to sputter desorption of reactants from the surface before they have time to react and/or lower dc-biases (lower ion energies) observed at higher ICP power. Once again, the GaN etch results were significantly slower than those obtained in our earlier studies.[28] Etch rates tracked identically with the Cl^+ (413 nm) and the Cl^0 (837.5 nm) emission intensity as determined by OES indicating that both the physical and

https://doi.org/10.1557/S1092578300003483 Published online by Cambridge University Press

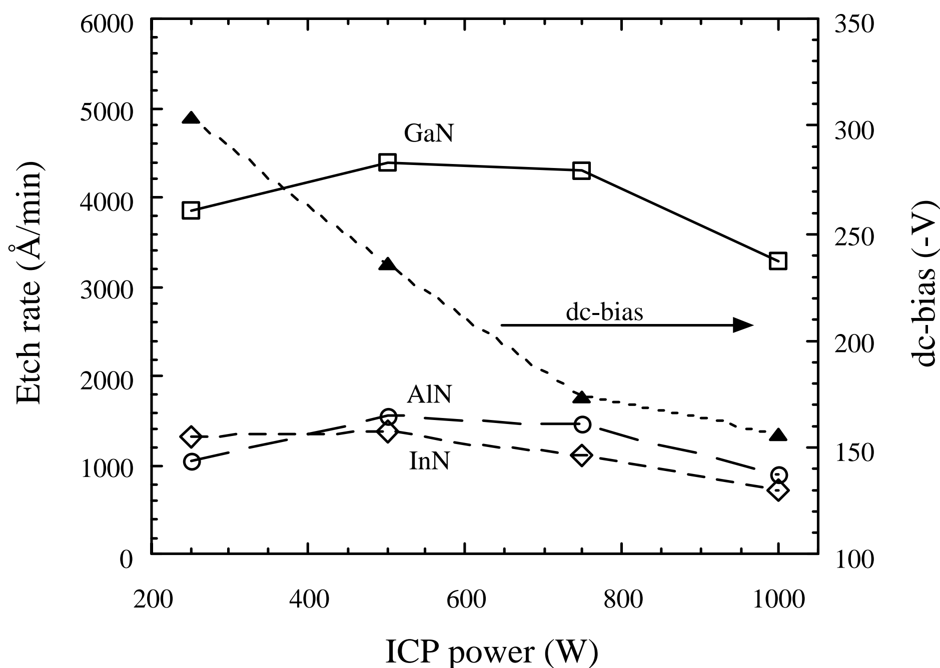

Figure 7. GaN, InN, and AlN etch rates as a function of ICP source power in a $BCl_3/Cl_2/Ar$ plasma. Plasma conditions were: 2 mTorr pressure, 125 W cathode rf-power with corresponding dc-bias ranging from –160 to –300 V, 32 sccm Cl_2, 8 sccm BCl_3, and 25°C cathode temperature.

chemical components of the etch are significant. Additional Cl^0 emission lines increased slightly with ICP source power. In Figure 8, GaN:AlN etch selectivity remained relatively constant, whereas the GaN:InN increased slightly with ICP power.

AFM was used to quantify the etched surface morphology as rms roughness for many of the plasma conditions reported in this paper. Rough etch morphology often indicates a non-stoichiometric surface due to preferential removal of either the group-III or group-V species. The rms roughness for the as-grown samples were 1.00 nm for GaN, 5.98 nm for AlN, and 239.97 nm for InN. For GaN, the surface morphology remained smooth, (< 5.1 nm) as a function of $\%Cl_2$, ICP source power, and cathode rf-power implying stoichiometric etching. RMS roughness for GaN, InN, and AlN is plotted as a function of $\%Cl_2$ concentration in Figure 9. The largest GaN rms roughness was obtained in pure BCl_3 where the physical component of the etch
was greatest due to higher mass ions and then remained relatively constant at < 1.7 nm as Cl_2 was added to the plasma. The InN rms was normalized to the as-grown rms and scanned over a 40 x 40 µm area (as compared to 10 x 10 µm for GaN and AlN) due to the as-grown sample's rough surfaces. The InN surface remained relatively smooth as a function of plasma gas ratio again implying stoichiometric etching. However, the AlN rms roughness increased to a maximum of 34.2 nm at 50% Cl_2 and then smoothed out as the Cl_2 concentration increased. This trend may be attributed to the high bonding energy for AlN and demonstrates the need to balance the chemical-to-physical ratio of the etch mechanism.

https://doi.org/10.1557/S1092578300003483 Published online by Cambridge University Press

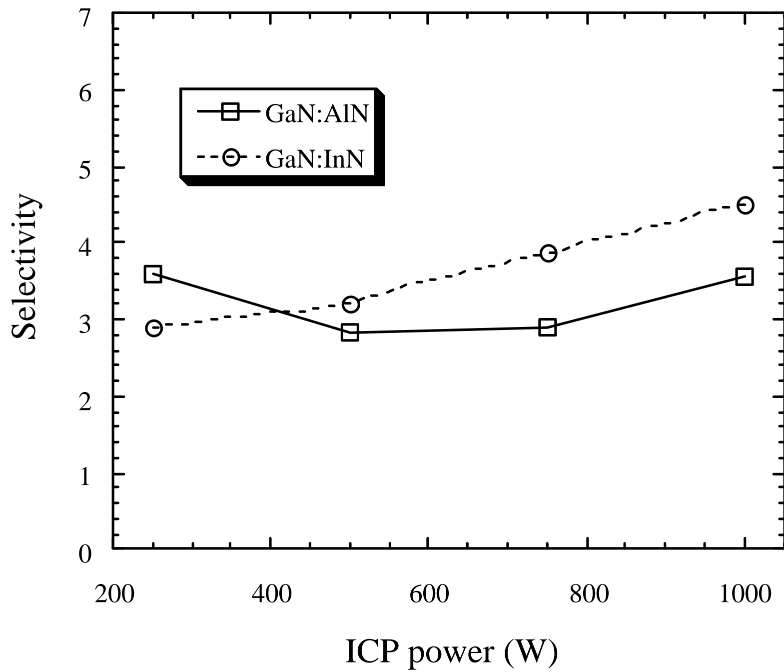

Figure 8. GaN:AlN and GaN:InN etch selectivities as a function of ICP source power in a $BCl_3/Cl_2/Ar$ plasma. Plasma conditions were: 2 mTorr pressure, 125 W cathode rf-power with corresponding dc-bias ranging from –160 to –300 V, 32 sccm Cl_2, 8 sccm BCl_3, and 25°C cathode temperature.

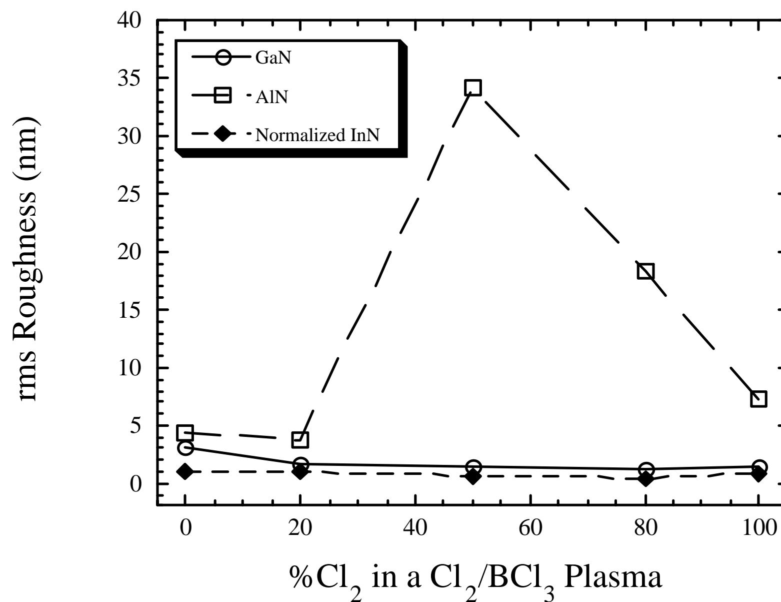

Figure 9. GaN, AlN, and normalized InN rms roughness as a function of $\%Cl_2$. ICP etch conditions were 32 sccm Cl_2, 8 sccm BCl_3, 5 sccm Ar, 500 W ICP source power, and 2 mTorr pressure.

https://doi.org/10.1557/S1092578300003483 Published online by Cambridge University Press

In general, etch profiles ranged from highly anisotropic and smooth to undercut and rough dependent upon the plasma etch conditions. For example, in Figure 10, SEM micrographs are shown for GaN samples etched at a) -50, b) -150, and c) -300 V dc-bias under the following conditions; 32 sccm Cl_2, 8 sccm BCl_3, 5 sccm Ar, 500 W ICP source power, and 2 mTorr pressure. The etch anisotropy improved as the dc-bias increased from -50 to -150 V dc-bias due to the perpendicular nature of the ion bombardment energies. However, at -300 V dc-bias a tiered etch profile with vertical striations in the sidewall was observed due to erosion of the mask-edge under high ion bombardment energies. GaN etch profiles declined as either the ion energy or plasma flux increased. This was attributed to breakdown of the mask edge. For InN and AlN the range of plasma conditions yielding anisotropic smooth etching was much less than GaN. This trend may be attributed to GaN being more reactive in Cl-based plasmas, higher quality of as-grown material, low volatility of the InN etch products, or the higher bonding energy of AlN.

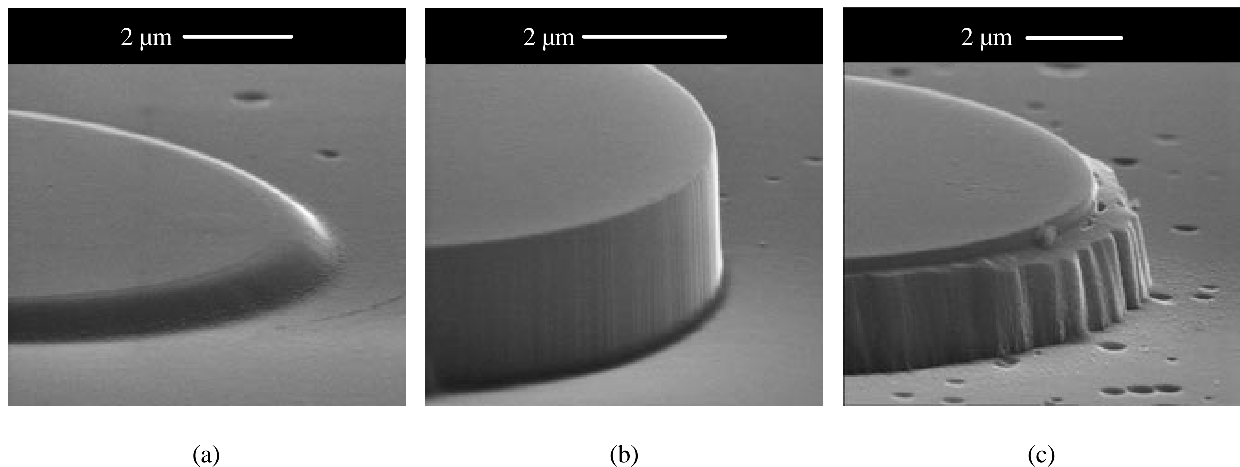

(a) (b) (c)

Figure 10. SEM micrographs for GaN etched at a) -50, b) -150, and c) -300 V dc-bias. ICP etch conditions were 32 sccm Cl_2, 8 sccm BCl_3, 5 sccm Ar, 500 W ICP power, and 2 mTorr pressure.

CONCLUSIONS

In summary, the BCl_3/Cl_2 plasma chemistry appears to provide a very versatile etch process for the group-III nitrides. However, the etch selectivity for GaN:AlN and GaN:InN is typically low < 7:1 as a function of $\%Cl_2$ in a Cl_2/BCl_3 plasma, ICP source power, and cathode rf-power. Selectivity seemed to improve as the concentration of reactive Cl increased due to the strong dependence of the GaN etch rate on the neutral and ion Cl flux which had very little effect on AlN and InN. Etch selectivity for the group-III nitrides was much less dependent on ion-to-neutral flux and ion energy. A wide range of plasma conditions were observed which yielded highly anisotropic etch profiles with smooth etch morphologies for GaN with a more limited range for InN and AlN.

ACKNOWLEDGMENTS

Sandia is a multiprogram laboratory operated by Sandia Corporation, a Lockheed Martin Company, for the United States Department of Energy under contract DE-ACO4-94AL85000. Two of the authors (L. F. Lester and L. Zhang) are also supported by a National Science Foundation CAREER Grant EC5-9501785.

https://doi.org/10.1557/S1092578300003483 Published online by Cambridge University Press

REFERENCES

1. I. Adesida, A. Mahajan, E. Andideh, M. Asif Khan, D. T. Olsen, and J. N. Kuznia, Appl. Phys. Lett. 63, 2777 (1993).
2. M. E. Lin, Z. F. Zan, Z. Ma. L. H. Allen, and H. Morkoç, Appl. Phys. Lett. 64, 887 (1994).
3. A. T. Ping, I. Adesida, M. Asif Khan, and J. N. Kuznia, Electron. Lett. 30, 1895 (1994).
4. H. Lee, D. B. Oberman, and J. S. Harris, Jr., Appl. Phys, Lett. 67, 1754 (1995).
5. S. J. Pearton, C. R. Abernathy, F. Ren, J. R. Lothian, P. W. Wisk, A. Katz, and C. Constantine, Semicond. Sci. Technol. 8, 310 (1993).
6. S. J. Pearton, C. R. Abernathy, and F. Ren, Appl. Phys. Lett. 64, 3643 (1994).
7. R. J. Shul, S. P Kilcoyne, M. Hagerott Crawford, J. E. Parmeter, C. B. Vartuli, C. R.
8. L. Zhang, J. Ramer, J. Brown, K. Zheng, L. F. Lester, S. D. Hersee, Appl. Phys. Lett. 68, 367 (1996).
9. B. Humphreys and M. Govett, MIJNSR 1, (1996).
10. R. J. Shul, G. B. McClellan, S. A. Casalnuovo, D. J. Rieger, S. J. Pearton, C. Constantine, C. Barratt, R. F. Karlicek, Jr., C. Tran, and M. Schurman, Appl. Phys. Lett. 69, 1119 (1996).
11. C. B. Vartuli, S. J. Pearton, J. W. Lee, J. D. MacKenzie, C. R. Abernathy, and R. J. Shul, J. Vac. Sci. and Technol B15, 98 (1997).
12. C. B Vartuli, S. J. Pearton, J. D. MacKenzie, C. R. Abernathy, and R. J. Shul, J. Electrochem. Soc. 143, L246 (1996).
13. J. Hong, T. Maeda, S. M. Donovan, J. D. MacKenzie, C. R. Abernathy, S. J. Pearton, R. J. Shul, and J. Han, MIJNSR 3, 5 (1998).
14. S. J. Pearton, C. R. Abernathy, and F. Ren, Appl. Phys. Lett. 64, 2294 (1994).
15. R. J. Shul, C. I. H. Ashby, D. J. Rieger, A. J. Howard, S. J. Pearton, C. R. Abernathy, C. B. Vartuli, P. A. Barnes, and P. Davis, Mat. Res. Soc. Symp. Proc. Vol. 395, 751 (1996).
16. J. W. Lee, J. Hong, and S. J. Pearton, Appl. Phys. Lett. 68, 847 (1996).
17. C. Constantine, C. Barratt, S. J. Pearton, F. Ren, and J. R. Lothian, Electron. Lett. 28, 1749 (1992).
18. C. Constantine, C. Barratt, S. J. Pearton, F. Ren, and J. R. Lothian, Appl. Phys. Lett. 61, 2899 (1992).
19. D. G. Lishan and E. L. Hu, Appl. Phys. Lett. 56, 1667 (1990).
20. Hyun Cho, J. Hong, T. Maeda, S. M. Donovan, C. R. Abernathy, S. J. Pearton, R. J. Shul, and J. Han, J. Electron. Mats. 27, 915 (1998).
21. S. A. Smith, C. A. Wolden, M. D. Bremser, A. D. Hanser, and R. F. Davis, Appl. Phys. Lett. 71, 3631, 1997.
22. C. B. Vartuli, S. J. Pearton, J. D. MacKenzie, C. R. Abernathy, and R. J. Shul, J. Electrochem. Soc. 143, L246 (1996).
23. J. W. Lee, Hyun Cho, D. C. Hays, C. R. Abernathy, S. J. Pearton, R. J. Shul, G. A. Vawter, and J. Han, IEEE J. of Selected Topics in Quantum Electronics, 4, 557 (1998).
24. R. J. Shul, C. G. Willison, M. M. Bridges, J. Han, J. W. Lee, S. J. Pearton, C. R. Abernathy, J. D. MacKenzie, S. M. Donovan, L. Zhang, and L. F. Lester, J. Vac. Sci. Technol A16, 1621 (1998).
25. R. J. Shul, C. G. Willison, M. M. Bridges,. J. Han, J. W. Lee, S. J. Pearton, C. R. Abernathy, J. D. MacKenzie, S. M. Donovan, Mat. Res. Soc. Symp. Proc. Vol. 483, 155 (1998).
26. J. W. Lee, J. Hong, and S. J. Pearton, Appl. Phys. Lett. **68**, 847 (1996).
27. Y. H. Lee, H. S. Kim, W. S. Kwon, G. Y. Yeom, J. W. Lee, M. C. Yoo, and T. I. Kim, J. Vac. Sci. Technol. A16, 1478 (1998).
28. R. J. Shul, C. I. H. Ashby, C. G. Willison, L. Zhang, J. Han, M. M. Bridges, S. J. Pearton, J. W. Lee, and L. F. Lester, Mats. Res. Soc. Symp. Proc. 512, 487 (1998).

https://doi.org/10.1557/S1092578300003483 Published online by Cambridge University Press